Polaritons in a Polycrystalline Layer of Non-fullerene Acceptor

Citation for published version (APA):
Liu, L., Wei, Z., & Meskers, S. C. J. (2023). Polaritons in a Polycrystalline Layer of Non-fullerene Acceptor. *Journal of the American Chemical Society*, *145*(4), 2040-2044. https://doi.org/10.1021/jacs.2c11968

Document license:
CC BY

DOI:
10.1021/jacs.2c11968

Document status and date:
Published: 01/02/2023

Document Version:
Publisher's PDF, also known as Version of Record (includes final page, issue and volume numbers)

Please check the document version of this publication:

• A submitted manuscript is the version of the article upon submission and before peer-review. There can be important differences between the submitted version and the official published version of record. People interested in the research are advised to contact the author for the final version of the publication, or visit the DOI to the publisher's website.
• The final author version and the galley proof are versions of the publication after peer review.
• The final published version features the final layout of the paper including the volume, issue and page numbers.

Link to publication

General rights
Copyright and moral rights for the publications made accessible in the public portal are retained by the authors and/or other copyright owners and it is a condition of accessing publications that users recognise and abide by the legal requirements associated with these rights.

- Users may download and print one copy of any publication from the public portal for the purpose of private study or research.
- You may not further distribute the material or use it for any profit-making activity or commercial gain
- You may freely distribute the URL identifying the publication in the public portal.

If the publication is distributed under the terms of Article 25fa of the Dutch Copyright Act, indicated by the "Taverne" license above, please follow below link for the End User Agreement:

www.tue.nl/taverne

Take down policy
If you believe that this document breaches copyright please contact us at:

openaccess@tue.nl

providing details and we will investigate your claim.

Download date: 05. Oct. 2023

JOURNAL OF THE AMERICAN CHEMICAL SOCIETY
pubs.acs.org/JACS
Communication

Polaritons in a Polycrystalline Layer of Non-fullerene Acceptor

Lixuan Liu, Zhixiang Wei,* and Stefan C. J. Meskers*

Cite This: J. Am. Chem. Soc. 2023, 145, 2040−2044
Read Online

ABSTRACT: Non-fullerene acceptor molecules developed for organic solar cells feature a very intense absorption band in the near-infrared. In the solid phase, the strong interaction between light and the transition dipole moment for molecular excitation should induce formation of polaritons. The reflection spectra for polycrystalline films of a non-fullerene acceptor with a thienothienopyrrolo-thienothienoindole core of the so-called Y6 type indeed show a signature of polaritons. A local minimum in the middle of the reflection band is associated with the allowed molecular transition. The minimum in reflection allows efficient entry of light into the solid, resulting in a local maximum in external quantum efficiency of a photovoltaic cell made of the pure acceptor.

Polaritons are the quanta of light inside matter.[1,2] A polariton is a quantum mechanical hybrid between a photon and an excitation in a material. The hybridization results from strong coupling between the excitation and resonant electromagnetic waves.[3] Such strong coupling can be enforced by the confinement of light in an optical cavity incorporating also molecular material.[4−6] Through the formation of such cavity polaritons, many amazing feats have been accomplished: low threshold lasing,[6−9] optical transistors operating down to the single-quantum level,[10−13] and external control over the rates of thermal chemical reactions inside the cavity.[14] Strong coupling between light and matter can also be induced in the bulk condensed phase by tightly packing oriented dye molecules with large oscillator strength in, e.g., a molecular crystal or an aggregate.[13,15] A spectroscopic signature of such bulk polaritons is the local minimum in the middle of the reflection band associated with an allowed electronic transition of the material.[16]

To support this view, we illustrate in Figure 1 the occurrence of this minimum for a variety of semiconductors. The explanation of the minimum is still under debate. It has been attributed to vibrations coupling with the excitation[17,18] but has also been related directly to the dispersion relation of the polaritons.[16] To see this, we first approximate the imaginary part of the refractive index or absorption by a delta function of frequency:

$$\kappa(\omega) = \frac{\pi}{2}\frac{\omega_P^{\ 2}}{\omega_D}\delta(\omega - \omega_D) \tag{1}$$

with ω_D the resonance frequency of the allowed transition. ω_P denotes the plasma frequency, given by

$$\omega_P^{\ 2} = Nfq_e^{\ 2}/\varepsilon_0 m_e \tag{2}$$

where N is the number of molecules per unit volume, f the oscillator strength, ε_0 the permittivity of vacuum, q_e the electron charge, and m_e the mass.[27]

Applying the Kramers−Kronig transform,[28,29] we directly obtain for the frequency dependence of the refractive index:

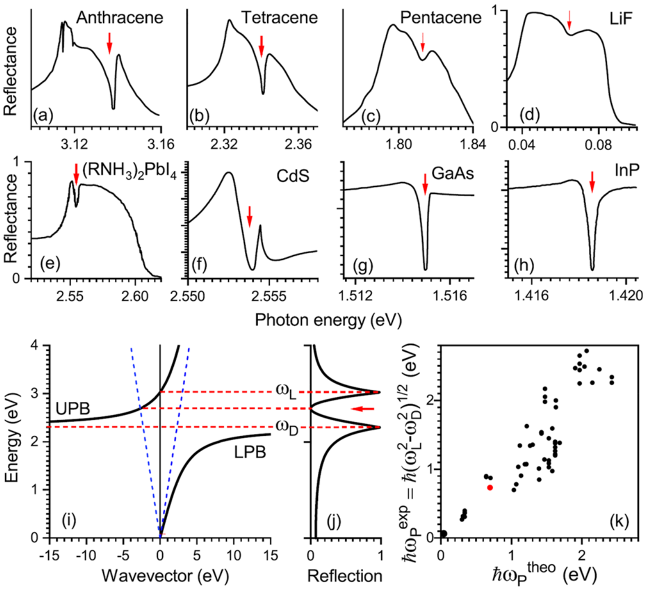

Figure 1. Experimental reflection spectra of organic and inorganic semiconductors as reported in the literature: (a) T = 2 K, (001), $E\|\mathbf{b}$;[19] (b) 2 K, (001), $E\|\mathbf{b}$;[20] (c) 1.85 K, (001), $E\|\mathbf{b}$;[21] (d) 2 K, (001), $E\|\mathbf{b}$, $k\|\mathbf{c}$;[22] (e) 4 K, $E\perp\mathbf{c}$, $k\|\mathbf{c}$, R = $H_{21}C_{10}$;[23] (f) 2 K, (100);[24] (g) 2 K;[25] and (h) 4 K.[26] (i) Dispersion relation based on eq 2. (j) Reflection based on the dispersion relation. (k) Experimental versus predicted energy quanta associated with the plasma frequency. The red dot represents the result from this study.

Received: November 10, 2022
Published: January 23, 2023

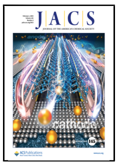

https://doi.org/10.1021/jacs.2c11968

$$n(\omega) = 1 + \frac{{\omega_P}^2}{{\omega_D}^2 - \omega^2} \tag{3}$$

Multiplying $n(\omega)$ with ω, we get the dispersion relation for the polariton with its characteristic upper and lower polariton branches (UPB and LPB); see Figure 1i. The reflection of light under normal incidence, $R(\omega) = ((1 - n(\omega))/(1 + n(\omega)))^2$, features two maxima, one at $\omega = \omega_D$ and the other at $\omega_L = ({\omega_D}^2 + {\omega_P}^2)^{1/2}$, with a minimum in between; see Figure 1j. The minimum occurs at the frequency where the UPB crosses the photon line, i.e., where the electromagnetic waves in the material travel at the same phase velocity as in vacuum and therefore can enter the material unimpeded. The two maxima in reflection allow us to determine experimentally a value for the plasma frequency via $\omega_P = ({\omega_L}^2 - {\omega_D}^2)^{1/2}$. This value can then be compared to a theoretical prediction via eq 2. In Figure 1k we compare experimental and theoretical estimates for the energy quanta associated with the plasma frequency for a set of molecular crystals based on literature data (see Supporting Information (SI) for details).

The correlation between experimental and predicted values illustrates the usefulness of the polariton concept for understanding the optical properties of molecular crystals.[30,31] Yet surprisingly little experimental evidence has appeared indicating a role for polaritons in organic optoelectronic devices.[32] This may be related to the fact that often the molecular layers used are amorphous.[33−35] Here we investigate a polycrystalline film of the non-fullerene acceptor (*S*,*S*)-BTP-4F (**1**).[36,37] We show that, while for amorphous films hardly any polariton characteristics are observable, for thermally annealed polycrystalline films the reflection spectrum shows a pronounced minimum in the middle of the lowest band.

Solutions of **1** in chloroform feature an intense absorption centered around 732 nm, with decadic absorption coefficient $\varepsilon = 0.979 \times 10^5$ M^{-1} cm^{-1}, and are characterized by an oscillator strength $f = 0.7$ and a transition dipole moment $\mu_{01} = 10.2$ D; see Figure 2.

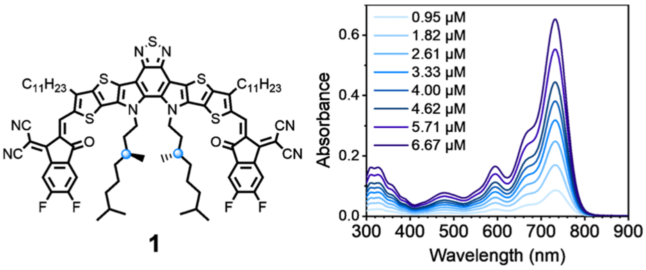

Figure 2. Structure of **1** and its absorption spectrum in chloroform at various concentrations with an optical pathlength of 1 cm.

Thermal annealing of a spin-coated layer of **1** results in a polycrystalline film; see Figure 3.[38,39] Inspection of the domains of the film between parallel polarizers reveals a pronounced dichroism across the visible spectrum, indicating that all molecules are aligned in the same direction. Between crossed polarizers, the films show the expected birefringence associated with molecules aligned in the plane of the film. X-ray diffraction of a single crystal indicates packing of molecules in quasi-two-dimensional layers, separated by the long alkyl sidechains on the molecules.[40−45] Within the quasi-2D layers, the dye molecules pack in a brickwork arrangement, with the transition dipole moments for the lowest allowed transition all pointing in the same direction.[46]

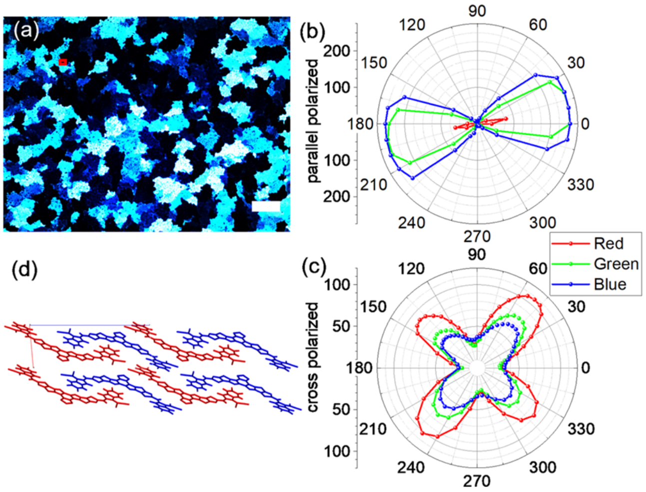

Figure 3. (a) Polarizing optical microscope image of a thermally annealed film of **1** between parallel polarizers. Scale bar: 40 μm. (b, c) Polar diagrams for (b) the transmitted red, green, and blue light for a single crystalline domain between parallel polarizes and (c) crossed polarizers. (d) Packing of molecules in quasi-2D layers in a crystal of **1**.

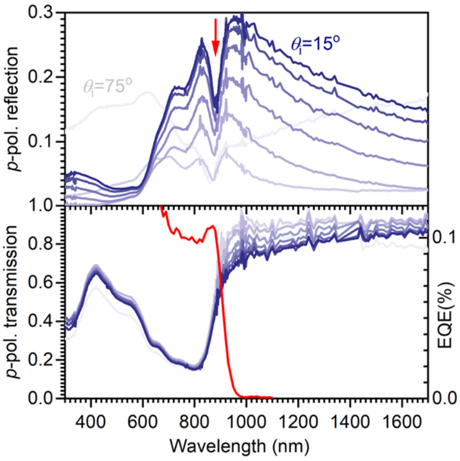

Figure 4. (Top) *p*-polarized reflection for a polycrystalline film of **1** annealed at 290 °C for various angles of incidence θ_i from 15° to 75°. (Bottom) *p*-polarized transmission (blue) for θ_i from 0° to 70° and external quantum efficiency (EQE, red) from a photovoltaic cell glass/ITO/ZnO/**1**/MoO$_3$/Ag/sputtered ITO under 1 sun illumination, thermally annealed at 110 °C.

The polycrystalline film of **1** strongly reflects light with wavelength near 900 nm, with reflection close to 30% for near normal incidence; see Figure 4. Looking at the reflection graph starting at the long-wavelength side, we see an incease of the reflectivity with decreasing wavelength. This is to be expected because we approach the allowed lowest absorption band near 800 nm (see Figure 2), with the refractive index increasing sharply. Upon increasing the angle of incidence θ_i, the reflectivity for *p*-polarized light at long wavelengths first decreases and then increases again for $\theta_i > 70°$. This is consistent with the known vanishing reflectivity for *p*-polarized light when incident under the Brewster angle. The reflection spectrum shows a first maximum for light with wavelength $\lambda =$

952 nm and a second extremum at λ = 830 nm, with in between the characteristic minimum at λ = 875 nm. From the maxima we estimate $\hbar\omega_P$ = 0.73 eV. Using the oscillator strength f for **1** in solution and the number density in the crystal from X-ray diffraction, eq 2 predicts $\hbar\omega_P$ = 0.70 eV.

Films annealed at a lower temperature (110 vs 290 °C) show smaller domains. The reflection spectra for these films show maxima at the same characteristic wavelength but with a minimum that is less deep; see SI. Preliminary data on the relation between the depth of the reflection minimum and the typical lateral size of the crystalline domains indicate a lateral coherence length up to 35 μm for the polaritons generated in the film via the minimum in reflection (Figure S13).

Films annealed at 110 °C remain closed so that diodes without electrical shorts can be fabricated with a layer of **1** as semiconducting medium. We use semitransparent contacts to minimize any optical cavity effects. These diodes show a small but significant photovoltaic effect and generate photocurrent under simulated sunlight of about 1 sun intensity, with an external quantum efficiency (EQE) under short circuit exceeding 0.1% for light with wavelength around 800 nm; see Figure 4, bottom. The EQE spectrum shows a local maximum near 875 nm that coincides with the minimum in reflection for film annealed at 110 °C. From this we conclude that the local minimum in the reflection band allows light to enter the semiconducting molecular layer efficiently and to contribute to photocurrent generation.

In conclusion, polycrystalline films of **1** show the characteristic feature of polaritons in their reflection spectrum. The local minimum in the lowest reflection band allows efficient entry of light at the onset of the absorption band despite the refractive index in this region. This shows that polariton effects should be considered when evaluating optoelectronic properties of molecular semiconductors.

ASSOCIATED CONTENT

Supporting Information

The Supporting Information is available free of charge at https://pubs.acs.org/doi/10.1021/jacs.2c11968.

> Experimental section, database of reflection spectra and crystal structure, crystallographic parameters of **1**, photovoltaic parameters, absorption coefficient in solution, optical microscope images, transmission and reflection spectra for films, EQE spectra, the dependence of relative depth of the reflection minimum on the lateral domain size, and GIWAXS patterns of thermally annealed films (PDF)

Accession Codes

CCDC 2154787 contains the supplementary crystallographic data for this paper. These data can be obtained free of charge via www.ccdc.cam.ac.uk/data_request/cif, or by emailing data_request@ccdc.cam.ac.uk, or by contacting The Cambridge Crystallographic Data Centre, 12 Union Road, Cambridge CB2 1EZ, UK; fax: +44 1223 336033.

AUTHOR INFORMATION

Corresponding Authors

Zhixiang Wei − *CAS Key Laboratory of Nanosystem and Hierarchical Fabrication, National Center for Nanoscience and Technology, Beijing 100190, China; School of Future Technology, University of Chinese Academy of Sciences, Beijing 100049, China;* orcid.org/0000-0001-6188-3634; Email: weizx@nanoctr.cn

Stefan C. J. Meskers − *Molecular Materials and Nanosystems, Institute for Complex Molecular Systems, Eindhoven University of Technology, Eindhoven 5600 MB, The Netherlands;* orcid.org/0000-0001-9236-591X; Email: s.c.j.meskers@tue.nl

Author

Lixuan Liu − *Molecular Materials and Nanosystems, Institute for Complex Molecular Systems, Eindhoven University of Technology, Eindhoven 5600 MB, The Netherlands; CAS Key Laboratory of Nanosystem and Hierarchical Fabrication, National Center for Nanoscience and Technology, Beijing 100190, China; School of Future Technology, University of Chinese Academy of Sciences, Beijing 100049, China;* orcid.org/0000-0002-2781-9601

Complete contact information is available at: https://pubs.acs.org/10.1021/jacs.2c11968

Notes

The authors declare no competing financial interest.

ACKNOWLEDGMENTS

The authors acknowledge the financial support from the Ministry of Science and Technology of China (Grant no. 2021YFA1200303), the National Natural Science Foundation of China (Grant nos. 21721002 and 22135001), the Strategic Priority Research Program of Chinese Academy of Sciences (No. XDB36000000), and the China Scholarship Council (202104910462).

REFERENCES

(1) Hopfield, J. J. Theory of the Contribution of Excitons to the Complex Dielectric Constant of Crystals. *Phys. Rev.* **1958**, *112* (5), 1555−1567.

(2) Pekar, S. I. Theory Theory of electromagneitc waves in a crystal with excitons. *J. Phys. Chem. Solids* **1958**, *5* (1−2), 11−22.

(3) Mills, D. L.; Burstein, E. Polaritons-Electromagnetic modes of media. *Rep. Prog. Phys.* **1974**, *37* (7), 817−926.

(4) Lidzey, D. G.; Bradley, D. D. C.; Skolnick, M. S.; Virgili, T.; Walker, S.; Whittaker, D. M. Strong exciton-photon coupling in an organic semiconductor microcavity. *Nature* **1998**, *395* (6697), 53−55.

(5) Kasprzak, J.; Richard, M.; Kundermann, S.; Baas, A.; Jeambrun, P.; Keeling, J. M. J.; Marchetti, F. M.; Szymanska, M. H.; Andre, R.; Staehli, J. L.; Savona, V.; Littlewood, P. B.; Deveaud, B.; Dang, L. S. Bose−Einstein condensation of exciton polaritons. *Nature* **2006**, *443* (7110), 409−414.

(6) Kena-Cohen, S.; Forrest, S. R. Room-temperature polariton lasing in an organic single-crystal microcavity. *Nat. Photonics* **2010**, *4* (6), 371−375.

(7) Plumhof, J. D.; Stoferle, T.; Mai, L. J.; Scherf, U.; Mahrt, R. F. Room-temperature Bose−Einstein condensation of cavity exciton-polaritons in a polymer. *Nat. Mater.* **2014**, *13* (3), 247−252.

(8) Schneider, C.; Rahimi-Iman, A.; Kim, N. Y.; Fischer, J.; Savenko, I. G.; Amthor, M.; Lermer, M.; Wolf, A.; Worschech, L.; Kulakovskii, V. D.; Shelykh, I. A.; Kamp, M.; Reitzenstein, S.; Forchel, A.; Yamamoto, Y.; Hofling, S. An electrically pumped polariton laser. *Nature* **2013**, *497* (7449), 348−352.

(9) Bhattacharya, P.; Xiao, B.; Das, A.; Bhowmick, S.; Heo, J. Solid State Electrically Injected Exciton-Polariton Laser. *Phys. Rev. Lett.* **2013**, *110* (20), 206403.

(10) Zasedatelev, A. V.; Baranikov, A. V.; Urbonas, D.; Scafirimuto, F.; Scherf, U.; Stöferle, T.; Mahrt, R. F.; Lagoudakis, P. G. A room-temperature organic polariton transistor. *Nat. Photonics* **2019**, *13* (6), 378−383.

(11) Gao, T.; Eldridge, P. S.; Liew, T. C. H.; Tsintzos, S. I.; Stavrinidis, G.; Deligeorgis, G.; Hatzopoulos, Z.; Savvidis, P. G. Polariton condensate transistor switch. *Phys. Rev. B* **2012**, *85* (23), 235102.

(12) Ballarini, D.; De Giorgi, M.; Cancellieri, E.; Houdre, R.; Giacobino, E.; Cingolani, R.; Bramati, A.; Gigli, G.; Sanvitto, D. All-optical polariton transistor. *Nat. Commun.* **2013**, *4*, 1778.

(13) Tang, J.; Zhang, J.; Lv, Y.; Wang, H.; Xu, F. F.; Zhang, C.; Sun, L.; Yao, J.; Zhao, Y. S. Room temperature exciton-polariton Bose–Einstein condensation in organic single-crystal microribbon cavities. *Nat. Commun.* **2021**, *12* (1), 3265.

(14) Thomas, A.; Lethuillier-Karl, L.; Nagarajan, K.; Vergauwe, R. M. A.; George, J.; Chervy, T.; Shalabney, A.; Devaux, E.; Genet, C.; Moran, J.; Ebbesen, T. W. Tilting a ground-state reactivity landscape by vibrational strong coupling. *Science* **2019**, *363* (6427), 615–619.

(15) Pandya, R.; Chen, R. Y. S.; Gu, Q. F.; Sung, J.; Schnedermann, C.; Ojambati, O. S.; Chikkaraddy, R.; Gorman, J.; Jacucci, G.; Onelli, O. D.; Willhammar, T.; Johnstone, D. N.; Collins, S. M.; Midgley, P. A.; Auras, F.; Baikie, T.; Jayaprakash, R.; Mathevet, F.; Soucek, R.; Du, M.; Alvertis, A. M.; Ashoka, A.; Vignolini, S.; Lidzey, D. G.; Baumberg, J. J.; Friend, R. H.; Barisien, T.; Legrand, L.; Chin, A. W.; Yuen-Zhou, J.; Saikin, S. K.; Kukura, P.; Musser, A. J.; Rao, A. Microcavity-like exciton-polaritons can be the primary photoexcitation in bare organic semiconductors. *Nat. Commun.* **2021**, *12* (1), 6519.

(16) Meskers, S. C. J.; Lakhwani, G. Reflection of light by anisotropic molecular crystals including exciton-polaritons and spatial dispersion. *J. Chem. Phys.* **2016**, *145* (19), 194703.

(17) Alvertis, A. M.; Pandya, R.; Quarti, C.; Legrand, L.; Barisien, T.; Monserrat, B.; Musser, A. J.; Rao, A.; Chin, A. W.; Beljonne, D. First principles modeling of exciton-polaritons in polydiacetylene chains. *J. Chem. Phys.* **2020**, *153* (8), 084103.

(18) Weiser, G.Strong Exciton Polaritons in Anisotropic Crystals: Macroscopic Polarization and Exciton Properties. *Photophysics of Molecular Materials: From Single Molecules to Single Crystals*; Wiley-VCH: Weinheim, Germany, 2005; pp 429–496.

(19) Turlet, J. M.; Philpott, M. R. Reflection spectrum of first singlet transition of crystalline anthracene at low temperature. *J. Chem. Phys.* **1975**, *62* (7), 2777–2781.

(20) Turlet, J. M.; Philpott, M. R. Surface and bulk exciton-transitions in refelction spectrum of tertracene. *J. Chem. Phys.* **1975**, *62* (11), 4260–4265.

(21) Piryatinski, Y. P.; Kurik, M. V. Influence of structural defects on excitonic photoluminescence of pentacene. *Ukr. J. Phys.* **2011**, *56* (10), 1048–1055.

(22) Hirasawa, M.; Ishihara, T.; Goto, T.; Sasaki, S.; Uchida, K.; Miura, N. Magnetoreflection of the lowest exciton in a layeres perovskite-type compound. *Solid State Commun.* **1993**, *86* (8), 479–483.

(23) Hopfield, J. J.; Thomas, D. G. Theoretical and Experimental Effects of Spatial Dispersion on the Optical Properties of Crystals. *Phys. Rev.* **1963**, *132* (2), 563–572.

(24) Sell, D. D.; Stokowski, S. E.; Dingle, R.; DiLorenzo, J. V. Polariton Reflectance and Photoluminescence in High-Purity GaAs. *Phys. Rev. B* **1973**, *7* (10), 4568–4586.

(25) Evangelisti, F.; Fischbach, J. U.; Frova, A. Dependence of exciton reflectance on field and other surface characteristics: The case of InP. *Phys. Rev. B* **1974**, *9* (4), 1516–1524.

(26) Jasperse, J. R.; Kahan, A.; Plendl, J. N.; Mitra, S. S. Temperature Dependence of Infrared Dispersion in Ionic Crystals LiF and MgO. *Phys. Rev.* **1966**, *146* (2), 526–542.

(27) Smith, D. Y., Dispersion theory, Sum rules, and their Application to analysis of optical data. In *Handbook of optical constants of solids*; Palik, E. D., Ed.; Elsevier, 1997; Vol *1*.

(28) Nussenzveig, H. M.*Causality and Dispersion Relations*; Academic Press: New York, 1972; pp 3–53.

(29) Ashcroft, N. W.; Mermin, N. D.*Solid State Physics*. Brooks/Cole; Belmont, 1976; pp 778–779.

(30) Kim, J. H.; Schembri, T.; Bialas, D.; Stolte, M.; Wurthner, F. Slip-Stacked J-Aggregate Materials for Organic Solar Cells and Photodetectors. *Adv. Mater.* **2022**, *34* (22), 2104678.

(31) Zhong, X.; Chervy, T.; Zhang, L.; Thomas, A.; George, J.; Genet, C.; Hutchison, J. A.; Ebbesen, T. W. Energy Transfer between Spatially Separated Entangled Molecules. *Angew. Chem. Int. Ed.* **2017**, *56* (31), 9034–9038.

(32) Wang, M.; Hertzog, M.; Börjesson, K. Polariton-assisted excitation energy channeling in organic heterojunctions . *Nat. Commun.* **2021**, *12* (1), 1874.

(33) DelPo, C. A.; Khan, S. U.; Park, K. H.; Kudisch, B.; Rand, B. P.; Scholes, G. D. Polariton Decay in Donor-Acceptor Cavity Systems. *J. Phys. Chem. Lett.* **2021**, *12* (40), 9774–9782.

(34) Shen, Z.; Jiang, Y.; Yu, J.; Zhu, Y.; Bu, L.; Lu, G. Film-Depth-Dependent Light Reflection Spectroscopy for Photovoltaics and Transistors. *Adv. Mater. Interfaces* **2021**, *8* (22), 2101476.

(35) Ma, X.; Zeng, A.; Gao, J.; Hu, Z.; Xu, C.; Son, J. H.; Jeong, S. Y.; Zhang, C.; Li, M.; Wang, K.; Yan, H.; Ma, Z.; Wang, Y.; Woo, H. Y.; Zhang, F. Approaching 18% efficiency of ternary organic photovoltaics with wide bandgap polymer donor and well compatible Y6: Y6–1O as acceptor. *Natl. Sci. Rev.* **2021**, *8* (8), nwaa305.

(36) Liu, L.; Wei, Z.; Meskers, S. C. J. Semi-Transparent, Chiral Organic Photodiodes with Incident Direction-Dependent Selectivity for Circularly Polarized Light. *Adv. Mater.* **2023**, 2209730.

(37) Liu, L.; Yang, Y.; Zhu, L.; Zhang, J.; Chen, K.; Wei, Z. Chiral Non-Fullerene Acceptor Enriched Bulk Heterojunctions Enable High-Performance Near-Infrared Circularly Polarized Light Detection. *Small* **2022**, *18* (31), 2202941.

(38) Xiao, Y.; Yuan, J.; Zhou, G.; Ngan, K. C.; Xia, X.; Zhu, J.; Zou, Y.; Zhao, N.; Zhan, X.; Lu, X. Unveiling the crystalline packing of Y6 in thin films by thermally induced "backbone-on" orientation. *J. Mater. Chem. A* **2021**, *9* (31), 17030–17038.

(39) Li, X. N.; Lu, H. P.; Zhu, W. G. Recent Advances in Y6-Based Semiconductors: Performance in Solar Cells, Crystallography, and Electronic Structure. *ChemPlusChem.* **2021**, *86* (5), 700–708.

(40) Lin, F.; Jiang, K.; Kaminsky, W.; Zhu, Z.; Jen, A. K. Y. A Non-fullerene Acceptor with Enhanced Intermolecular pi-Core Interaction for High-Performance Organic Solar Cells. *J. Am. Chem. Soc.* **2020**, *142* (36), 15246–15251.

(41) Zhang, G.; Chen, X. K.; Xiao, J.; Chow, P. C. Y.; Ren, M.; Kupgan, G.; Jiao, X.; Chan, C. C. S.; Du, X.; Xia, R.; Chen, Z.; Yuan, J.; Zhang, Y.; Zhang, S.; Liu, Y.; Zou, Y.; Yan, H.; Wong, K. S.; Coropceanu, V.; Li, N.; Brabec, C. J.; Bredas, J. L.; Yip, H. L.; Cao, Y. Delocalization of exciton and electron wavefunction in non-fullerene acceptor molecules enables efficient organic solar cells. *Nat. Commun.* **2020**, *11* (1), 3943.

(42) Zhu, W.; Spencer, A. P.; Mukherjee, S.; Alzola, J. M.; Sangwan, V. K.; Amsterdam, S. H.; Swick, S. M.; Jones, L. O.; Heiber, M. C.; Herzing, A. A.; Li, G.; Stern, C. L.; DeLongchamp, D. M.; Kohlstedt, K. L.; Hersam, M. C.; Schatz, G. C.; Wasielewski, M. R.; Chen, L. X.; Facchetti, A.; Marks, T. J. Crystallography, Morphology, Electronic Structure, and Transport in Non-Fullerene/Non-Indacenodithienothiophene Polymer:Y6 Solar Cells. *J. Am. Chem. Soc.* **2020**, *142* (34), 14532–14547.

(43) Zhu, L.; Zhang, M.; Zhou, G.; Hao, T.; Xu, J.; Wang, J.; Qiu, C.; Prine, N.; Ali, J.; Feng, W.; Gu, X.; Ma, Z.; Tang, Z.; Zhu, H.; Ying, L.; Zhang, Y.; Liu, F. Efficient Organic Solar Cell with 16.88% Efficiency Enabled by Refined Acceptor Crystallization and Morphology with Improved Charge Transfer and Transport Properties. *Adv. Energy Mater.* **2020**, *10* (18), 1904234.

(44) Zhu, L.; Zhang, J.; Guo, Y.; Yang, C.; Yi, Y.; Wei, Z. Small Exciton Binding Energies Enabling Direct Charge Photogeneration Towards Low-Driving-Force Organic Solar Cells. *Angew. Chem., Int. Ed.* **2021**, *60* (28), 15348–15353.

(45) Li, C.; Zhou, J.; Song, J.; Xu, J.; Zhang, H.; Zhang, X.; Guo, J.; Zhu, L.; Wei, D.; Han, G.; Min, J.; Zhang, Y.; Xie, Z.; Yi, Y.; Yan, H.; Gao, F.; Liu, F.; Sun, Y. Non-fullerene acceptors with branched side chains and improved molecular packing to exceed 18% efficiency in organic solar cells. *Nat. Energy* **2021**, *6* (6), 605–613.

(46) Khan, M. U.; Hussain, R.; Yasir Mehboob, M.; Khalid, M.; Shafiq, Z.; Aslam, M.; Al-Saadi, A. A.; Jamil, S.; Janjua, M. In Silico Modeling of New "Y-Series"-Based Near-Infrared Sensitive Non-Fullerene Acceptors for Efficient Organic Solar Cells. *ACS Omega* **2020**, *5* (37), 24125−24137.